Potassium channels in rat prostate epithelial cells

Halima Ouadid-Ahidouch[a,*], Fabien Van Coppenolle[a], Xuefen Le Bourhis[b], Abdelmajid Belhaj[a], Natalia Prevarskaya[a]

[a] *Laboratoire de Physiologie Cellulaire, Université de Lille I, INSERM EPI 9938, 59655 Villeneuve d'Ascq Cedex, France*
[b] *Laboratoire de Biologie de Développement, Équipe Facteurs de Croissance, Université de Lille I, 59655 Villeneuve d'Ascq Cedex, France*

Received 27 July 1999

Abstract Voltage-dependent K^+ channels were identified and characterized in primary culture of rat prostate epithelial cells. A voltage-dependent, inactivating K^+ channel was the most commonly observed ion channel in both lateral and dorsal cells. The K^+ current exhibited a voltage threshold at −40 mV. Averaged half-inactivation potential ($V_{1/2}$) and the slope factor (k) values were −26 mV and 6, respectively. It showed a monoexponential decay with an inactivation time constant of about 600 ms at +60 mV. The deactivation time constant at −60 mV was 30 ms and the reversal potential was estimated at −80 mV, suggesting that current was carried by potassium ions. The scorpion venom peptides charybdotoxin (5 nM) and margatoxin (1 nM), inhibited K^+ current at all membrane potentials with a rapid and a slow reversibility respectively. Both tetraethylammonium (10 mM) and 4-aminopyridine (50 μM) reduced K^+ current by ∼40%. We conclude that plasma membranes of lateral and dorsal rat prostate epithelial cells contain Kv K^+ channels that have biophysical and pharmacological properties consistent with those of the Kv1.3 family.

Key words: Kv K^+ channel; Whole cell recording; Prostate

1. Introduction

Potassium channels in the plasma membranes of non-excitable cells play crucial roles in cell development, volume regulation, stabilization of membrane potential and cell proliferation [1–4]. A number of studies have suggested that Kv1.3 K^+ channels play a functional role in the onset of cellular events associated with both T and B lymphocyte activation. Thus, Kv1.3 K^+ channels are implicated in the proliferation and interleukin 2 secretion of human B lymphocytes [5]. Recent studies have demonstrated that K^+ channel activity is also a key determinant for cell progression through the G1 phase of mitosis [4]. Kv1.3 K^+ channels have been linked to progression through the G1 phase in T lymphocytes. Ca^{2+}-activated K^+ channels may also play a role in regulating progression through G1 in MCF-7 human mammary epithelial cells [6]. Several recent studies have reported that the factors which determine cell volume strongly influenced the mechanisms controlling cell proliferation [7–9].

In several cell types, enhanced K^+ channel gene expression or increased K^+ channel activity has been found to be associated with mitogenesis [10]. Rane [11] and Huang and Rane [12] showed that ras oncogene-transformed 3T3 fibroblasts had Ca^{2+}-activated K^+ channels not present in non-transformed cells. In other cell lines, Teulon et al. [13] found that renal tubule epithelial cells transformed by simian virus 40 had three new K^+ channel amplitudes in addition to the K^+ channels normally present. Skryma et al. [14] found a new non-inactivating voltage-activated K^+ channel in the androgen-dependent human cancer prostate cell line LNCaP. This channel was sensitive to tetraethylammonium (TEA) and directly and reversibly inhibited by a rise in intracellular Ca^{2+}. When these K^+ channels were blocked, thymidine incorporation and proliferation decreased [14]. Although the K^+ channels in the human prostate cancer cell line LNCaP have been studied in great detail, very little is known about ionic conductance in both human or rat normal prostate cells and their role in signal transduction or cell growth regulation. Therefore, we first performed a primary culture of the adult rat prostate and characterized the ionic channels in these cells.

Both lateral and dorsal rat prostate epithelial cells expressed K^+ channels with the same properties as those of the Kv1.3 family.

2. Materials and methods

2.1. Dissociation of prostate tissue for primary culture

The lateral and dorsal lobes of 10–14-week-old Wistar rats were removed, freed of connective tissue and cut with scissors into ∼1 cm^2 fragments. Tissue pieces were placed in 10 ml of a solution containing 500 units of collagenase (type XI, Sigma France) and 200 units of hyaluronidase (type X, Sigma France) and incubated for 90 min at 37°C. Cells were then washed three times by centrifugation at 1000 rpm for 15 min. Cells were suspended in 5 ml of the solution and incubated at 37°C in a humidified atmosphere of 5% CO_2 and 95% air. The culture medium was changed on days 3 and 5.

The lateral and dorsal cells were cultured in Eagle's minimum essential medium (EMEM) supplemented with 5% horse serum, 16 ng/ml insulin, 2 mM L-glutamine, 500 IU/ml penicillin, 500 IU/ml streptomycin, 10 ng/ml EGF, and 0.06% HEPES buffer, and maintained at 37°C in a humid atmosphere of 5% CO_2 in air.

2.2. Immunophenotyping of stromal and epithelial cells in primary culture

Monoclonal murine antibodies specific for the following proteins were used in this study: α-smooth muscle actin, vimentin, and pan-cytokeratin. Cells were plated in multichamber slides for immunocytochemical analysis. After ethanol fixation at 4°C, they were rinsed twice with PBS, then incubated with PBS containing 3% BSA (blocking solution) for 45 min at room temperature. Cells were incubated with primary antibodies overnight at 4°C, then with bridging goat anti-mouse immunoglobulin G, and lastly with peroxidase-antiperoxidase complex. The reaction product was revealed with diaminobenzidine tetrahydrochloride and hydrogen peroxidase. Cells were counterstained with Harris hematoxylin to facilitate identification of culture elements.

2.3. Whole-cell/patch-clamp technique

For electrophysiological analysis, cells were cultured in 35 mm petri dishes. The petri dishes were substituted every 30–45 min. Currents

*Corresponding author. Fax: (33) 3 20 43 40 66.
E-mail: halima.ouadid@univ-lille1.fr

PII: S0014-5793(99)01121-7

and membrane potential were recorded under voltage-clamp or current-clamp mode, respectively, with an Axopatch 200 B patch-clamp amplifier (Axon Instruments, Burlingame, CA, USA). pClamp software (ver. 6.03, Axon Instruments) and Labmaster hardware (Digidata 2000) were used to control voltage and to acquire and analyze data. The whole-cell mode of the patch-clamp technique was used with borosilicate fire-polished pipettes (A-M systems, Everette, WA, USA) with 3–5 MΩ resistance. Seal resistance was typically in the 10–20 GΩ range. We carefully compensated the series resistance. The maximum uncompensated series resistance was <10 MΩ during whole-cell recordings, so the voltage error was <5 mV for a current amplitude of 500 pA. Recordings where series resistance resulted in errors greater than 5 mV in voltage commands were discarded. Liquid-liquid junction potentials were compensated using the Axopatch internal circuit. Whole-cell currents were allowed to stabilize for 5 min before K^+ currents were measured. Currents were filtered at 2 kHz with the filter of the Axopatch amplifier. The P/4 subpulse correction of cell leakage and capacitance was used to study the outward K^+ currents.

Cells were allowed to settle in petri dishes placed at the opening of a 250 μm i.d. capillary for extracellular perfusions (MSC-200, Manual solution changer, Bio-Logic Instruments, France). The cell under investigation was continuously superfused with control or test solutions.

All electrophysiological experiments were performed at room temperature.

2.4. Analysis

In all experiments, cells were depolarized every 30 s from −60 mV to different test potentials for 200 ms. At each voltage, the conductance (G_K) was calculated as $I_{peak}/(V_m - E_K)$, where E_K calculated was −86 mV. For activation, G_K during each voltage was normalized to maximal value (G_{max} at +40 mV). To obtain the half-maximal voltage ($V_{1/2}$) and the slope factor (k) values for K^+ current activation, we fitted data to a Boltzmann equation: $G = G_{max}/(1 + \exp^{[(V - V_{1/2})/k]})$.

Experimental values are given as mean ± S.E.M. of n experiments.

2.5. Solutions

External and internal solutions had the following compositions (in mM): External: NaCl 140, KCl 5, $CaCl_2$ 2, $MgCl_2$ 2, HEPES 10, glucose 5, $NaHCO_3$ 4, Na_2HPO_4 0.3, KH_2PO_4 0.4, penicillin 0.16, streptomycin 0.068 at pH 7.4 (NaOH). Internal: KCl 150, $CaCl_2$ 0.05, HEPES 10, EGTA 1.1, $MgCl_2$ 2, at pH 7.2 (KOH). Osmolarities of bath and pipette solutions were 300–310 and 300 mosmol/l, respectively, measured with a freezing point depression osmometer.

Free Ca^{2+} concentrations for the solutions applied from the inner side of the membrane were buffered with 1.1 mM EGTA and calculated using Maxc Software (from Chris Patton, Hopkins Marine Station, Stanford University). For example, to produce 0.5 μM and 1 μM free Ca^{2+} solutions with (in mM): 0.826 $CaCl_2$, 2 $MgCl_2$, 1.1 EGTA and 0.944 $CaCl_2$, 2 $MgCl_2$, 1.1 EGTA were used respectively.

2.6. Chemicals

Margatoxin (MgTX) and charybdotoxin (ChTX) (Latoxan, France) were made up in BSA 1%, HEPES 5 mM (pH 7.2). Final concentrations were obtained by appropriate dilution in external control solution.

3. Results

3.1. Immunophenotyping of primary cell cultures derived from rat prostate lobes

Several studies have shown that prostate tissue is made up

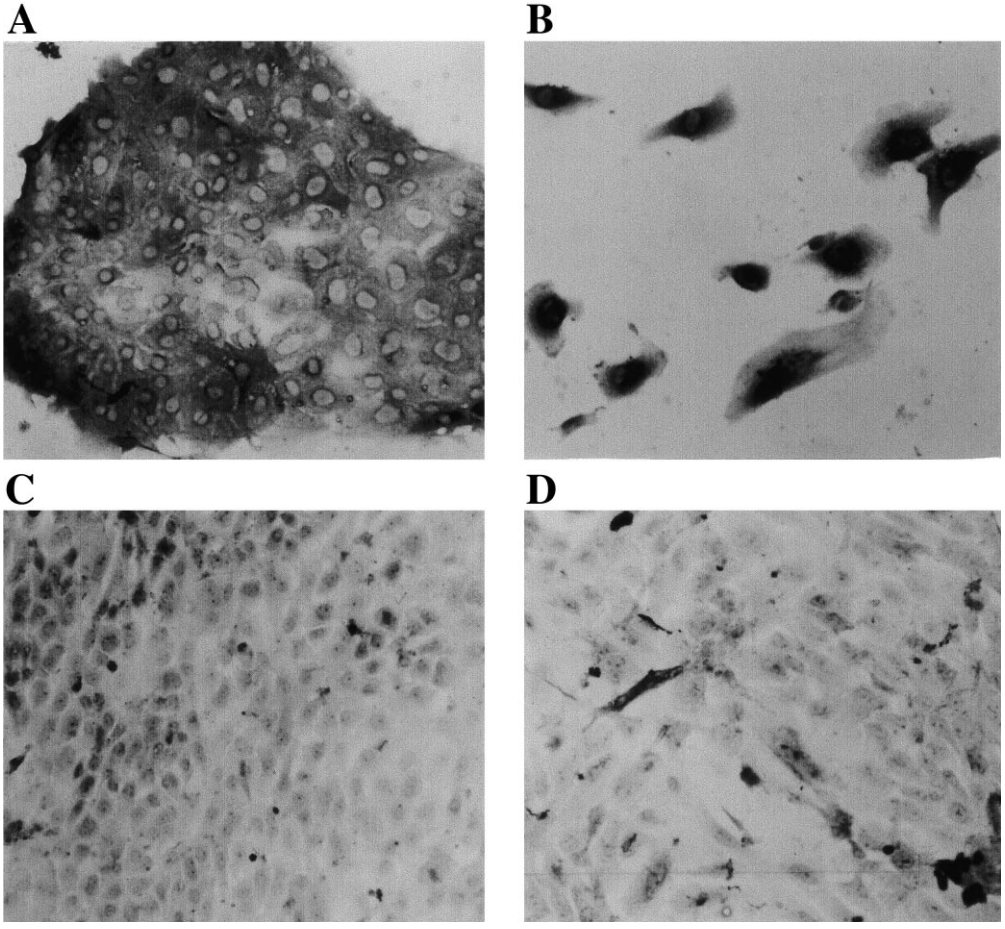

Fig. 1. Immunophenotyping of stromal and epithelial cells derived from the lateral lobe in primary culture. A: Epithelial cells were strongly positive for pan-cytokeratin. B: Isolated epithelial cells positive to pan-cytokeratin. Epithelial cells were negative for both α-actin (C) and vimentin (D).

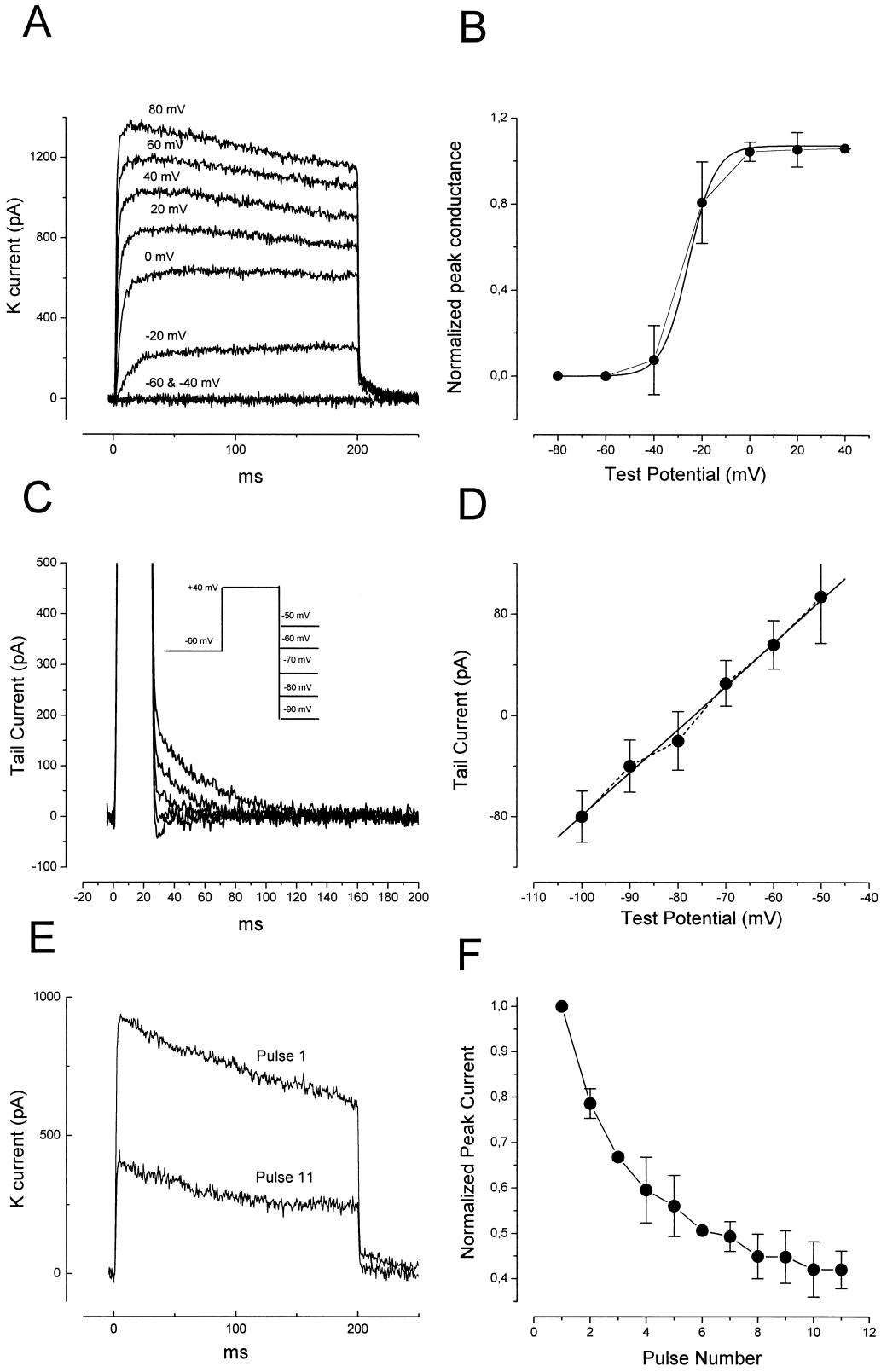

Fig. 2. Characterization of voltage-activated K^+ channel in lateral rat prostate epithelial cells. A: Examples of original K^+ currents obtained by stepping the membrane potential from −60 mV in 20 mV increments for 200 ms. B: Voltage dependence of activation. Activation curve was fitted to the Boltzmann equation (see Section 2.4). Means ± S.D. are shown ($n = 10$). C: Deactivation, tail currents after shifting to potentials of −90 to −50 mV following rapid activation to +40 mV at 30s intervals. D: Tail current-voltage relationship. E: Current was elicited by a series of 11 depolarizing voltage steps to +40 mV once every second from a holding potential of −60 mV. F: Mean normalized peak K^+ current during the series of depolarizing voltage steps (from −60 mV to +40 mV) at 1 s intervals.

of different types of cells: fibroblasts, smooth muscle, and epithelial cells [15–16]. The epithelial phenotype of cells in primary culture derived from lateral and dorsal rat lobes was verified by immunocytochemical assays. Fig. 1 shows the immunochemical staining of cells derived from lateral lobes. The majority of cells expressed pan-cytokeratin (Fig. 1A,B) but not anti-smooth muscle α-actin (Fig. 1C) or vimentin (anti-fibroblasts) (Fig. 1D). The epithelial phenotype of cells derived from dorsal rat lobe was also confirmed by immunocytochemical assays. A similar profile was observed (positive to pan-cytokeratin and negative to both α-actin and vimentin; data not shown).

3.2. Membrane potential and membrane capacitance of rat epithelial cells

Membrane potential obtained 5 min after accessing the intracellular compartment was -42 ± 4 mV ($n = 22$) and -40 ± 5 mV ($n = 25$) for lateral and dorsal epithelial cells, respectively. The whole-cell capacitance was 14 ± 3 pF ($n = 10$) for lateral cells and 19 ± 6 pF ($n = 15$) for dorsal cells.

3.3. Whole-cell currents in prostate lateral cells

Currents were elicited with 200 ms depolarizing voltage steps from −60 mV to +80 mV in 20 mV increments (Fig. 2A). The outward current reached a peak within 9.6 ± 0.68 ms ($n = 10$) and then slowly inactivated. The activation time constant (measured at +60 mV) was 1.5 ± 0.3 ms ($n = 10$). The outward currents appeared to present a single population of channels that activated at a depolarizing potential between −40 and −30 mV. The voltage dependence of this channel was determined by calculating normalized peak conductance values from the peak current amplitudes at different potentials and fitting them to a Boltzmann function (see Section 2.4). The average $V_{1/2}$ and k were -26 ± 4 mV ($n = 10$) and 5.5 ± 0.6 ($n = 10$), respectively (Fig. 2B). Moreover, the mean outward current density was 76 ± 38 pA/pF at +60 mV ($n = 10$).

To identify the reversal potential and, therefore, the ionic nature of the outward current, we studied tail currents following repolarization to different test potentials. As shown in Fig. 2C, the tail current following a 15 ms conditioning pulse to +40 mV test pulse was clearly inward at −90 mV and outward at −70 mV. From the current-voltage relationship of the tail currents, the reversal potential of the outward current was estimated to be -77 ± 6 mV ($n = 7$, Fig. 2D). The reversal potential was close to the K^+ equilibrium potential calculated under our conditions ($E_K = -86$ mV), suggesting that the outward current was predominantly carried by K^+ ions. Channel deactivation provides another convenient property for distinguishing between different types of K^+ channel. The time constant measured at −60 mV ranged from 21 to 50 ms with a mean of 30 ± 2 ms ($n = 11$). The time constant of inactivation ranged from 500 to 700 ms with a mean of 642 ± 79 ms ($n = 7$).

Inactivation of certain K^+ channels accumulates during repetitive depolarizing pulses delivered at 1 Hz because recovery during the inter-pulse interval is incomplete. This property was visualized as a reduction in current amplitude. The application of repetitive depolarization to K^+ channels induced a reduction in the amplitude of I_K ($63 \pm 14\%$, $n = 12$, Fig. 2E). The normalized peak current rapidly diminished (Fig. 2F). Thus, this channel exhibited a cumulative inactivation like that of Kv1.3.

The pharmacological profile provides a further test for defining Kv1.3 channels. We used two toxins known to inhibit Kv1.3 channels: a selective inhibitor (margatoxin, MgTX) and a less selective one (charybdotoxin, ChTX).

MgTX, a peptide purified from venom of the *Centruroides margaritatus* scorpion, blocks a brain Kv1.3 channel with a K_d of 50 pM in electrophysiological experiments [17,18]. The only other Shaker-like K^+ channel that was sensitive to MgTX is Kv1.6, but it is blocked with a 100-fold lower potency [17,18]. Originally, ChTX was reported to specifically block current through Ca^{2+}-activated K^+ channels in skeletal muscle [19]. In recent years, however, it has become clear that this toxin can also block voltage-gated K^+ channels [17,18] including Kv1.3 [20].

The extracellular perfusion of MgTX (1 nM) completely inhibited the outward current (Fig. 3A). The effect of MgTX reached a maximum at 6 min and was partially reversible after 15 min washing (Fig. 3B). The current-voltage relationships are shown in Fig. 3C. MgTX inhibited I_K at all potentials. The extracellular perfusion of ChTX (5 nM) reduced the amplitude of I_K by 73% (Fig. 3D, $66 \pm 2\%$, $n = 6$). In contrast to the effect of MgTX, the effect of ChTX on K^+ channels was immediate and completely reversible (Fig. 3E). Like MgTX, ChTX reduced I_K at all potentials (Fig. 3F). Moreover, ChTX used at 50 nM almost totally inhibited I_K ($87 \pm 3\%$, $n = 5$, data not shown).

We also tested the effect of other K^+ channel blockers: TEA and 4-aminopyridine (4-AP). These were already known to inhibit several types of K^+ channels, including Kv channels, in various cell types [18]. TEA (10 mM) and 4-AP (50 μM) reduced the K^+ channel amplitude by $43 \pm 7\%$ ($n = 6$) and $42 \pm 6\%$ ($n = 5$), respectively (data not shown).

3.4. Whole-cell currents in prostate dorsal cells

In dorsal epithelial cells, voltage steps from a holding po-

Table 1
Comparison of the biophysical properties of Kv1.3

	K^+ current in prostate cells	Kv1.3	Reference
Activation			
$V_{1/2}$	-26 ± 4	−21 mV	[32]
		−26 mV	[31]
		−35 mV	[33]
k	5.5	5.9	[32]
		7	[31]
Deactivation	30 ± 1.9	46 ms	[32]
		39 ms	[31]
Inactivation	600 ms	256.5 ms	[32]
Cumulative inactivation	Yes	Yes	

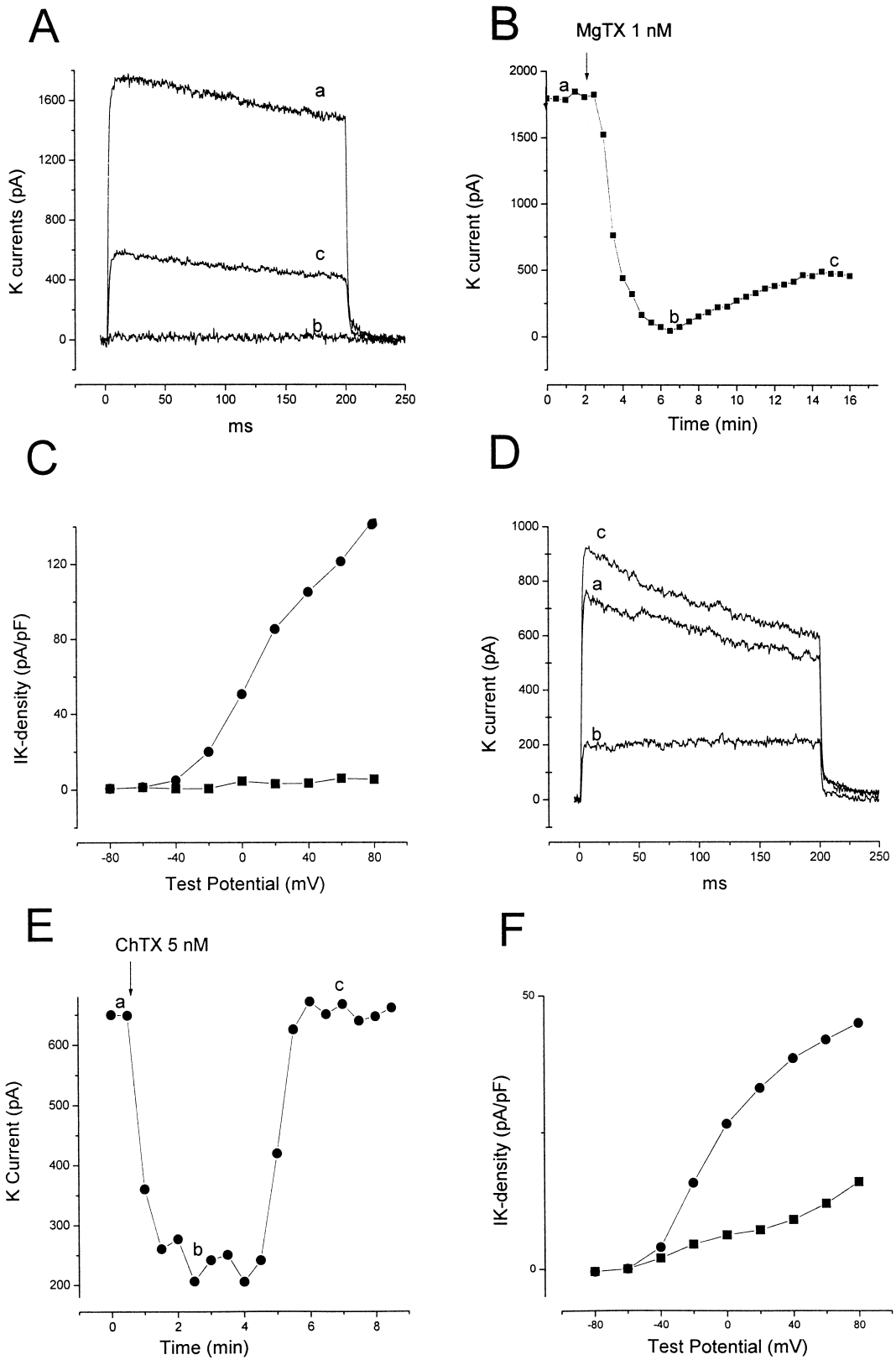

Fig. 3. Pharmacological characteristics of the K^+ current in cells derived from the lateral lobe. A: Individual K^+ current traces evoked by a depolarizing pulse from −60 mV to +60 mV, (a) I_K recorded in the control solution, (b) 6 min after 1 nM MgTX perfusion and (c) 10 min after MgTX wash. B: Time course of the K^+ current recorded in the control and after 1 nM MgTX application. C: Current-voltage relationship in the absence (●) and presence (■) of 1 nM MgTX. D: Individual current traces recorded from −60 mV to +60 mV, (a) I_K control, (b) I_K in the presence of 5 nM ChTX and (c) wash of ChTX. E: Time course of the K^+ current in the control and after 5 nM ChTX application. F: Current-voltage relationship in the absence (●) and presence (■) of 5 nM ChTX.

tential of −60 mV to +80 mV in 20 mV increments lasting 200 ms elicited an outward current that activated between −40 and −30 mV and inactivated. Average $V_{1/2}$ and k values were −26 ± 3 mV and 6 ± 0.8 (n = 9), respectively. Inactivation time constant measured at +60 mV ranged from 400 ms to 680 ms, with a mean of 568 ± 116 ms (n = 15). The mean deactivation time constant (measured at −60 mV) was 28 ± 2 ms (n = 6).

Like their counterparts recorded in lateral epithelial cells, the K^+ currents exhibited cumulative inactivation during the 200 ms depolarizing pulses to +40 mV from a holding potential of −60 mV, repeated once per second (data not shown).

K^+ current was also completely inhibited by 1 nM MgTX (n = 8) and reduced by 5 nM ChTX (65 ± 7%, n = 6, data not shown).

We also tested the effect of the increase of free $[Ca^{2+}]_i$ on K^+ current. In both lateral and dorsal epithelial cells, the increase of internal free Ca^{2+} to 0.5 μM or 1 μM (see Section 2.5 for free Ca^{2+} calculation) has no effect on the peak of K^+ current for periods of up to 15 min (n = 10).

4. Discussion

4.1. Immunophenotyping of primary cell cultures derived from rat prostate lobes

The rat prostate gland is composed of several distinct lobes: ventral, dorsal, lateral, and anterior (also called the coagulating gland) [21]. Each prostatic lobe is different in its morphology, secretions and response to hormones. The dorsolateral lobes (i) give rise to spontaneous and experimental tumors with varied hormone responsiveness [22], (ii) are considered to be the most homologous to the human prostate [21], and (iii) may play an important role in prostate cancer development [23,24]. Furthermore, the lateral lobe is considered to be the most hormone-sensitive part of the prostate [25,26].

In our studies, rat prostate cells derived from lateral or dorsal lobes retain cellular markers characteristic of epithelial cells. They expressed pan-cytokeratin but neither vimentin nor α-actin. Moreover, we report conditions that support the rapid, sustained proliferation of isolated normal prostate epithelial cells derived from the gland.

Different procedures of enzymatic digestion of rat ventral [16] or dorsolateral [15] prostates have been reported. To our knowledge, we were the first to culture the lateral and dorsal prostatic epithelial cells separately.

4.2. K^+ channels expressed in rat prostate epithelial cells

Our experiments demonstrated the existence of one type of K^+ channel in lateral and dorsal rat prostate epithelial cells. Essential properties of K^+ channels are: (i) voltage dependence (activated at −40 mV); (ii) cumulative inactivation; and (iii) high sensitivity to MgTX and ChTX, but moderate sensitivity to TEA.

The properties of the Kv channels expressed in lateral and dorsal prostate cells are consistent with the 'n' (normal) type described by Decoursey et al. [2]. N-type K^+ channels have been characterized in detail in human T lymphocytes, immature thymocytes, natural killer cells, murine thymocytes, and B lymphocytes [2,27–30].

We then compared the biophysical and pharmacological properties of the Kv1.3 channel in rat epithelial cells with those of cloned Kv1.3 expressed in mammalian cells [31,32] and *Xenopus* oocytes [33]. Further comparison was made with the activation, deactivation, and inactivation (see Table 1) of the native channel expressed in mouse or human T cells [3].

Thus, the K^+ currents expressed in both lateral and dorsal rat prostate epithelial cells closely resembled those expressed in *Xenopus* oocytes [33] or mammalian cells [31,32], as well as the native channels in mouse or human T cells.

However, the time constant of the inactivation of K^+ channels expressed in rat prostate cells was about two times slower than that of Kv1.3 (600 ms instead of 256 ms). Several studies have described that inactivation is slower with Cl (∼500 ms) than with others anions, especially fluoride (∼180 ms) [34,35].

The pharmacological profile provides a further test for defining K^+ channels in rat prostate cells. Both lateral and dorsal Kv1.3 channels, like their native Kv1.3 counterparts, are highly sensitive to the peptide toxins MgTX and ChTX, and moderately sensitive to TEA.

An inhibitory effect of $[Ca^{2+}]_i$ on Kv1.3 has been previously reported. Bregestovski et al. [36] observed a 4.5-fold reduction of current amplitude with pipette solutions buffered to 1 μM. However, the data reported by Verheugen [37] and Grissmer and Cahalan [38] show no effect of free $[Ca^{2+}]_i$ on the Kv1.3 current amplitude in physiological concentrations (< 10 μM) and even for concentrations as high as 2 mM. In our study, no inhibition of K^+ current by $[Ca^{2+}]_i$ with pipette solution buffered up to 1 μM of free Ca^{2+} was observed.

Thus, our results indicate that the biophysical and pharmacological properties of rat prostate K^+ channels are very similar to those of native Kv1.3 channels, except for the time constant of inactivation.

The physiological relevance of K^+ channels in normal prostate cells is questionable. Kv1.3 is involved in several physiological process: interleukin 2 secretion [5], cell proliferation [39], Ca^{2+} signaling [40], and cytotoxic killing [28]. Moreover, Kv1.3 channels are also involved in the K^+ efflux during the regulatory volume decrease that follows lymphocyte swelling [7]. There is a correlation with the level of endogenous Kv1.3 expression and the ability of mouse T cell lines to regulate volume [7]. Moreover, Kv1.3 is also implicated in promoting Ca^{2+} entry by maintaining the negative membrane potential [28]. In prostate cells, the Kv 1.3 K^+ channel may be a major determinant of the resting membrane potential that establishes the electrochemical driving force for Ca^{2+} influx. Furthermore, potassium channels are also associated with mitogenesis [10]. In the human prostate cancer cell line LNCaP, Skryma et al. [14] found a new non-inactivating voltage-activated K^+ channel which was sensitive to TEA and directly and reversibly inhibited by a rise in intracellular Ca^{2+}. Thus, we can also suggest that changes in the ion channel profiles may be linked to prostate cancer. However, the physiological role(s) of K^+ channel in prostate cells rest to determine.

The overall properties of the rat prostate epithelial cell K^+ channel suggest that it is a Kv 1.3-like K^+ channel. If this channel is specific to the prostate, as the *Slo3* channel is specific to the testis, pharmacological agents that target this K^+ channel may be useful in the study of prostate development. Further experiments using molecular biology techniques will be required to clone and study the expression of this channel in mammalian prostate cells.

Acknowledgements: This work was supported by la Région Nord-Pas de Calais, le Ministère de l'Education Nationale de l'Enseignement

Supérieur et de la Recherche, l'INSERM, l'Association de la Recherche contre le Cancer (ARC, France), and la Ligue contre le Cancer (France).

References

[1] Amigorena, S., Choquet, D., Teillaud, J.L., Korn, H. and Fridman, W.H. (1990) J. Immunol. 144, 2038–2045.
[2] Decoursey, T.E., Chandy, K.G., Gupta, S. and Cahalan, M.D. (1984) Nature 307, 465–468.
[3] Decoursey, T.E., Chandy, K.G., Gupta, S. and Cahalan, M.D. (1987) J. Gen. Physiol. 89, 379–404.
[4] Wonderlin, W.F. and Strobl, J.S. (1996) J. Membr. Biol. 154, 91–107.
[5] Price, M., Lee, S.C. and Deutsch, C. (1989) Proc. Natl. Acad. Sci. USA 86, 10171–10175.
[6] Ouadid-Ahidouch, H., Le Bhouris, X.F., Toiton, R.A. and Prevarskaya, N. (1998) J. Physiol. 513, 136P.
[7] Deutsch, C. and Chen, L.Q. (1993) Proc. Natl. Acad. Sci. USA 90, 10036–10040.
[8] Rouzaire-Dubois, B. and Dubois, J.M. (1998) J. Physiol. 510, 93–102.
[9] Grinstein, S. and Foskett, J.K. (1990) Annu. Rev. Physiol. 52, 399–414.
[10] Dubois, J.M. and Rouzaire-Dubois, B. (1993) Prog. Biophys. Mol. Biol. 59, 1–21.
[11] Rane, S.G. (1991) Am. J. Physiol. 260, C104–112.
[12] Huang, Y. and Rane, S.G. (1993) J. Physiol. 461, 601–618.
[13] Teulon, J., Ronco, P.M., Geniteau-Legendre, M., Baudouin, B., Estrade, S., Cassingena, R. and Vandewalle, A. (1992) J. Cell. Physiol. 151, 113–125.
[14] Skryma, R.N., Prevarskaya, N., Dufy-Barbe, L., Odessa, M.F., Audin, J. and Dufy, B. (1997) Prostate 33, 112–122.
[15] Nishi, N., Matuo, Y., Nakamoto, T. and Wada, F. (1988) In Vitro Cell Dev. Biol. 24, 778–786.
[16] Taketa, S., Nishi, N., Takasuga, H., Okutani, T., Takenaka, I. and Wada, F. (1990) Prostate 17, 207–218.
[17] Garcia, M.L., Knaus, H.G., Munujos, P., Slaughter, R.S. and Kaczorowski, J. (1995) Am. J. Physiol. 269, C1–C10.
[18] Garcia, M.L., Honner, M., Knaus, H.G., Koch, R., Schmalhofer, H., Slaughter, R.S. and Kaczorowski, G.J. (1997) Adv. Pharmacol. 39, 425–471.
[19] Miller, C., Moczydlowski, E., Latorre, R. and Phillips, M. (1985) Nature 313, 316–318.
[20] Sands, S.B., Lewis, R.S. and Cahalan, M.D. (1989) J. Gen. Physiol. 93, 1061–1074.
[21] Price, D. (1963) Natl. Cancer Inst. Monogr. 12, 351–369.
[22] Pollard, M. (1998) Prostate 36, 168–171.
[23] Janssen, T., Kiss, R. and Schulman, C. (1995) Acta Urol. Belg. 14, 7–14.
[24] Nevalainen, M.T., Valve, E.M., Ahonen, T., Yagi, A., Paranko, J. and Harkonen, P.L. (1997) FASEB J. 11, 1297–1307.
[25] Robinette, C. (1988) Prostate 12, 271–286.
[26] Schacht, M.J., Niederberger, C.S., Garnett, J.E., Sensibar, J.A., Lee, C. and Grayhack, J.T. (1992) Prostate 20, 51–58.
[27] Schlichter, L.C., Sidell, N. and Hagiwara, S. (1986) Proc. Natl. Acad. Sci. USA. 83, 5625–5629.
[28] Schlichter, L.C., Sidell, N. and Hagiwara, S. (1986) Proc. Natl. Acad. Sci. USA 83, 451–455.
[29] Choquet, D.C. and Korn, H. (1988) Biochem. Pharmacol. 37, 3797–3802.
[30] Lewis, R.S. and Cahalan, M.D. (1990) Annu. Rev. Physiol. 52, 415–430.
[31] Grissmer, S., Nguyen, A.N., Aiyar, J., Hanson, D.C., Mather, R.J., Gutman, G.A., Karmilowicz, M.J., Auperin, D.D. and Chandy, K.G. (1994) Mol. Pharmacol. 45, 1227–1234.
[32] Spencer, R.H., Sokolov, Y., Li, H., Takenaka, B., Milici, A.J., Aiyar, J., Nguyen, A., Park, H., Jap, B.K., Hall, J.E., Gutman, G.A. and Chandy, K.G. (1997) J. Biol. Chem. 272, 2389–2395.
[33] Grissmer, S., Dethlefs, B., Wasmuth, J.J., Goldin, A.L., Gutman, G.A., Cahalan, M.D. and Chandy, K.G. (1990) Proc. Natl. Acad. Sci. USA 87, 9411–9415.
[34] Cahalan, M.D., Chandy, K.G., Decoursey, T.E. and Gupta, S. (1985) J. Physiol. 358, 197–237.
[35] Verheugen, J.A.H., Oortgiesen, M. and Vijverberg, H.P.M. (1994) J. Membr. Biol. 137, 205–214.
[36] Bregestovski, P., Redkozubov, A. and Alexeev, A. (1986) Nature 319, 776–778.
[37] Verheugen, J.A.H. (1998) J. Physiol. 508, 167–177.
[38] Grissmer, S. and Cahalan, M.D. (1989) J. Gen. Physiol. 93, 609–630.
[39] Chandy, K.G., Decoursey, T.E., Cahalan, M.D., McLaughlin, C. and Gupta, S. (1984) J. Exp. Med. 160, 369–385.
[40] Lin, S., Boltz, R.C., Blake, J.T., Nguyen, M., Talento, A., Fisher, P.A., Springer, M.S., Sigal, N.H., Slaughter, R.S., Garcia, M.L., Kaczorowski, G.J. and Koo, G.C. (1993) J. Exp. Med. 177, 637–645.